FigureS1 related to Figure1

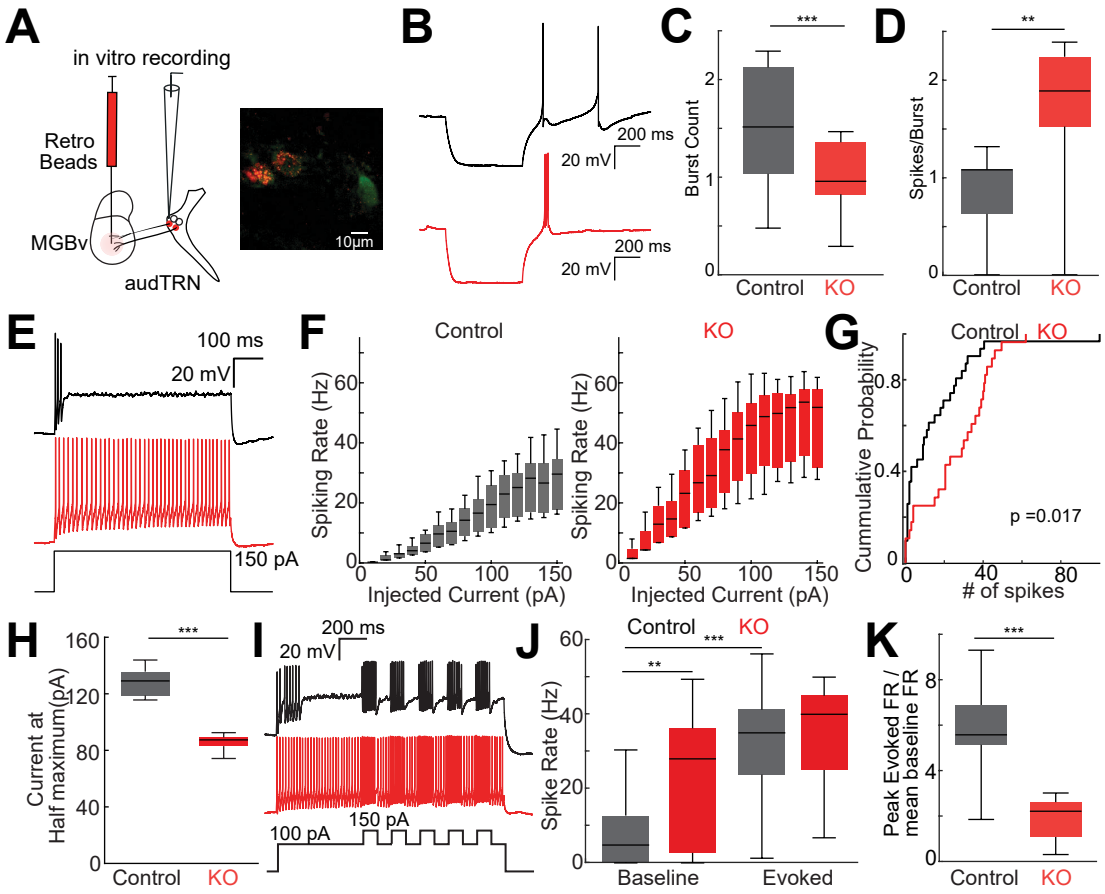

Figure S1: Changes in biophysical properties of audTRN in KO mice explain the loss in stimulus-related dynamic range. Related to Figure 1

A. (Left) Schematic of retrobeads based labeling approach used to identify audTRN neurons. (Right) Example confocal image showing retrobeads (red) in Ptchd1 expressing TRN neurons in Ptchd1-YFP+/- mouse. **B.** Representative voltage traces of whole cell recordings from identified control (black) and KO (red) audTRN neurons made in current clamp mode showing 'low-threshold' burst transients following a 500 ms hyperpolarizing current injection (0.5 nA, see methods). **C.** Boxplot showing the quantification of the median number of burst transients across recorded neurons. Significantly more burst events were observed in control compared with KO neurons (3 injections per cell, n = 31 control, 28 KO neurons; ***p < 0.001 rank-sum test). **D.** Boxplot showing the quantification of the median number of spikes crowning the first evoked burst-transient. Significantly more spikes were observed for KO compared with control neurons (3 injections per cell, n = 31 control, 28 KO neurons; **p < 0.01 rank-sum test). **E.** Example voltage trace showing the response of one control (top, black) and KO (red, bottom) audTRN neurons to injection of 150 pA inward current. **F.** Boxplots showing the distribution of spike rates for increasing current injections (10pA steps, 250 ms window) in control (left, black n=31 neurons) or KO (right, red, n=28 neurons) audTRN neurons **G.** Population data showing spike rates across recorded control (n = 31) or KO (n = 28) audTRN neurons for 150 pA inward current injection. **H.** Estimated current input required to reach the inflexion point (half maximum of the sigmoidal fit) based on multiple current injections in control and KO neurons (n = 31 control, m = 28 KO; ***p < 0.001 rank-sum). **I.** Example of a single control (black) or KO (red) voltage trace showing responses to a stepped current injection procedure (bottom). **J.** Firing rate following injection of 100 pA (Baseline) or after short pulse injections of 150 pA (Evoked). While evoked responses were comparable, baseline was significantly increased in the KO compared to controls (p < 1.3x10-13 Main Effect of genotype 1.0x10-7 Interaction, MANOVA; n = 15 control, m = 17 KO neurons; ** p <0.01 *** p < 0.001 rank-sum). **K.** Median dynamic ranges estimated from the procedure in I for control (n = 15 neurons) or KO (n = 17 neurons) audTRN neurons (***p < 0.001, rank-sum test).

Boxplots: median (line), quartiles (box), 95% confidence interval (whiskers)

FigureS2 related to Figure2

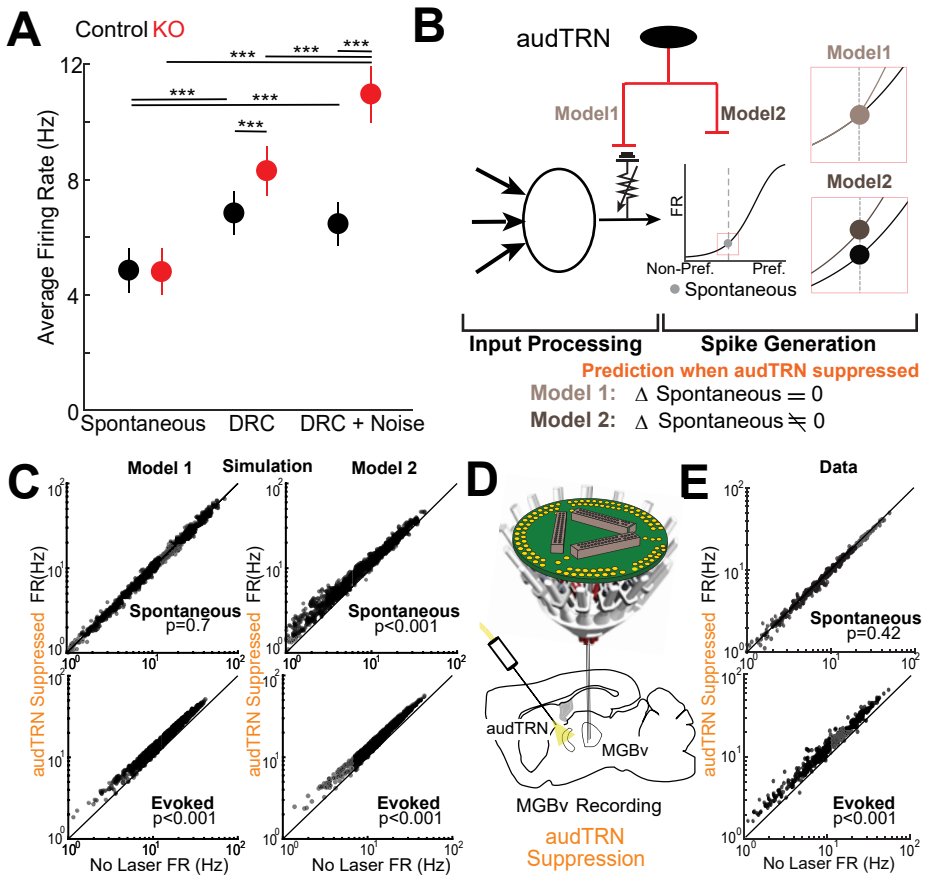

Figure S2: audTRN controls sensory-input gain of MGBv neurons. Related to Figure 2

A. Average firing rate of MGBv neurons during spontaneous (left), DRC stimulus (middle) or DRC with broadband noise added (right) in controls (black, N = 3 mice, 424 neurons) and KO (red, N = 3 mice, 235 neurons) animals (p< 1.6x10^-29 MANOVA Main Effects of stimulus, 1.3x10^-23 Interaction; *** p < 0.001 pairwise rank-sum test). Error bars show s.e.m. **B.** Diagram of 2 possible models for the influence of audTRN input on MGBv activity predicting 2 differential outcomes following audTRN suppression: If audTRN controls input integration, RF and spontaneous activity of MGBv neurons doesn't change but sound-evoked responses increase (Model 1). If audTRN controls output gain, both spontaneous and evoked responses increase (Model 2). **C.** Simulation results of Model 1 and 2 for spontaneous/evoked firing rates of MGBv neurons with/without audTRN suppression. (n = 1000 modelled units, sign-rank test). **D.** Schematic of multielectrode targeting of MGBv with optogenetic audTRN suppression. **E.** Population data for changes in spontaneous (top) and sound-evoked (bottom) responses of MGBv neurons with audTRN suppression. Spontaneous activity was unaffected while the evoked responses significantly increased with audTRN suppression. (N = 3 mice, 430 neurons, sign-rank test).

FigureS3 related to Figure3

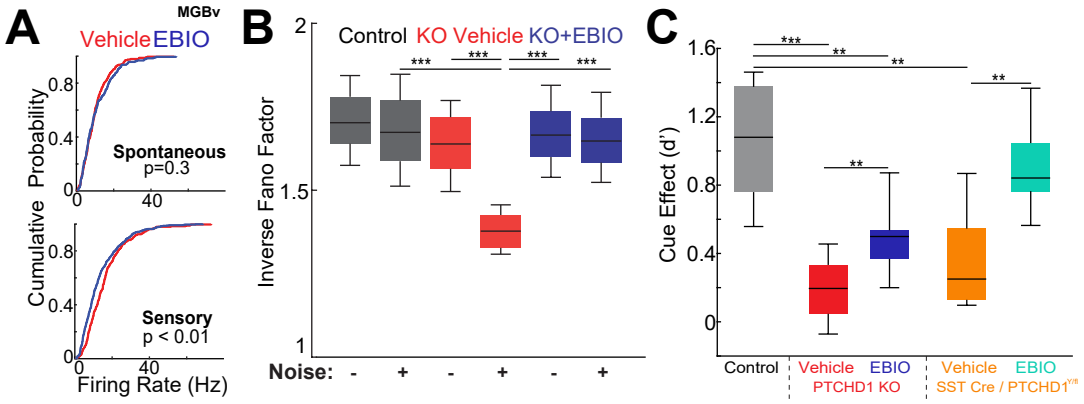

Figure S3: KO mice showed higher noise hypersensitivity. Related to Figure 3

A. Cumulative probability plot showing spontaneous (top) or sensory (bottom) response of MGBv neurons recorded across control (black, N = 3 mice, 424 neurons) and KO (red, N = 4 mice, 522 neurons) mice (Kolmogorov-Smirnov test). **B.** Inverse Fano factor values of MGBv neurons estimated across repeated presentations of dynamic random chords without or with background noise. Noise dependent decrease of response consistency in KO was rescued by injection of EBIO ($p<6.6\times10^{-28}$ MANOVA Main Effect of Genotype, $p < 3.1\times10^{-18}$ Interaction; 4 KO mice, n = 522 KO neurons; ***p<0.001, pairwise rank-sum test). **C.** Compared to global PTCHD1 KO, TRN specific PTCHD1 KO (SST Cre /PTCHD1y/fl; see methods) showed significantly higher cue-related behavioral improvement both with and without EBIO administration (N = 6 mice for control and KO and N=4 mice for SST Cre /PTCHD1y/fl, >10 sessions per condition; $p = 6.5\times10^{-73}$ MANOVA Main Effects, $p= 3.9\times10^{-10}$ Interaction; **p<0.01, ***p<0.001 pairwise rank-sum test with Bonferroni correction). Following EBIO, the cue effect in the TRN specific KO was not significantly different from control, suggesting that deficits in the cue effect seen in the full KO was due to the Ptchd1 deletion outside of TRN.

Boxplots: median (line), quartiles (box), 95% confidence interval (whiskers)

FigureS4 related to Figure4

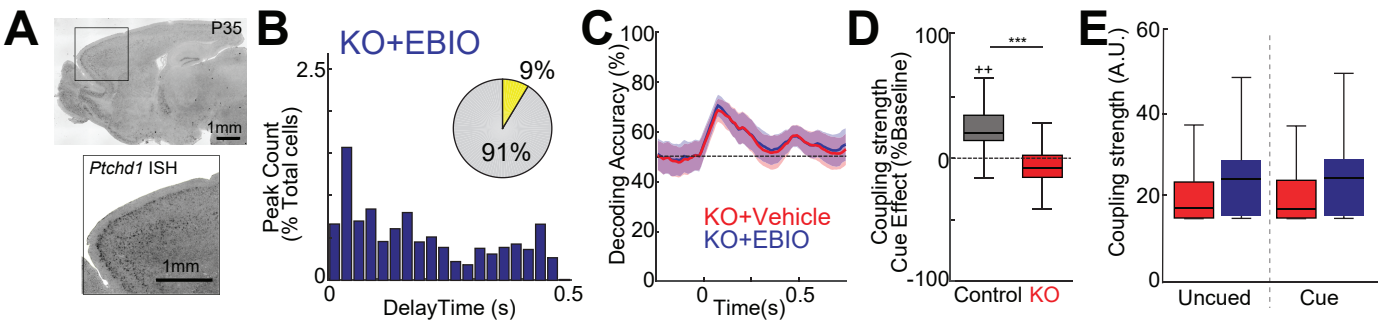

Figure S4: Deficits in cue representation maintenance in the PFC are not corrected by EBIO. Related to Figure 4

A. In situ hybridization showing the expression of PtchD1 in the PFC in adult (P35). **B.** Binned distribution of peak times for KO mice injected with EBIO as a percentage of total neurons. There was no significant increase in peak numbers following EBIO injection compared to the non-drug condition and so there were still significantly fewer peaks in KO mice compared with controls (totals for each genotype shown as inset pie-charts, yellow – peak cells; $p < 0.01$ Binomial test with Bonferroni Correction, N = 4 KO mice, n = 795 KO neurons recorded). **C.** Poisson naïve bayes decoding of predictive cue against unpredictive cue in KO mice following vehicle (red) or EBIO (blue) injection showing no improvement in decoding accuracy with EBIO. Decoding was limited to the 100 most strongly task modulated cells in the EBIO condition (see methods). Zero time indicates cue presentation (100msec duration). Shaded region indicates 95% confidence intervals. **D.** Boxplots comparing the coupling strength change associated with the cue for PFC neurons recorded from control (grey) or KO (red) mice. The cue consistently increased coupling for control but not KO (N = 4 control and 4 KO mice, n= 863 control and 947 KO neurons recorded, *** $p < 0.001$, pairwise rank-sum test; ++ $p < 0.01$ comparison from baseline) suggesting that behaviorally related changes in coupling were less effective in the KO. **E.** Quantification of the positive coupling strengths among regular spiking (RS) neurons (see methods) in KO mice during the delay period of uncued or cued trials following administration of vehicle (red) or EBIO (blue). Coupling was not affected by EBIO administration (see figure 4H for overall MANOVA, N = 4 KO mice, n = 795 KO neurons recorded; pairwise sign-rank test).

Boxplots: median (line), quartiles (box), 95% confidence interval (whiskers)

Table S1 related to Figure4

RS Cells

Genotype/Condition	Cell count	Rate	Error
Control/Vehicle	863	4.84	0.61
Control/Modafinil	863	4.74	0.92
KO/Vehicle	1742	5.19	0.95
KO/Modafinil	947	4.94	1.14
KO/EBIO	795	5.09	1.15

FS Cells

Genotype/Condition	Cell count	Rate	Error
Control/Vehicle	177	8.7	1.25
Control/Modafinil	177	11.33	1.43
KO/Vehicle	345	3.72	1.67
KO/Modafinil	183	9.29	1.43
KO/EBIO	162	5.17	1.9

Table S1: Firing rate comparison of PFC neurons in control and KO mice.

Related to Figure 4

Table showing average firing rates across recordings for PFC neurons identified as either regular spiking (RS) or fast spiking (FS) based on waveform characteristics (see methods). The error values shown are the standard error of the mean for each group. Rates were calculated during the delay period across trials.

FigureS5 related to Figure5

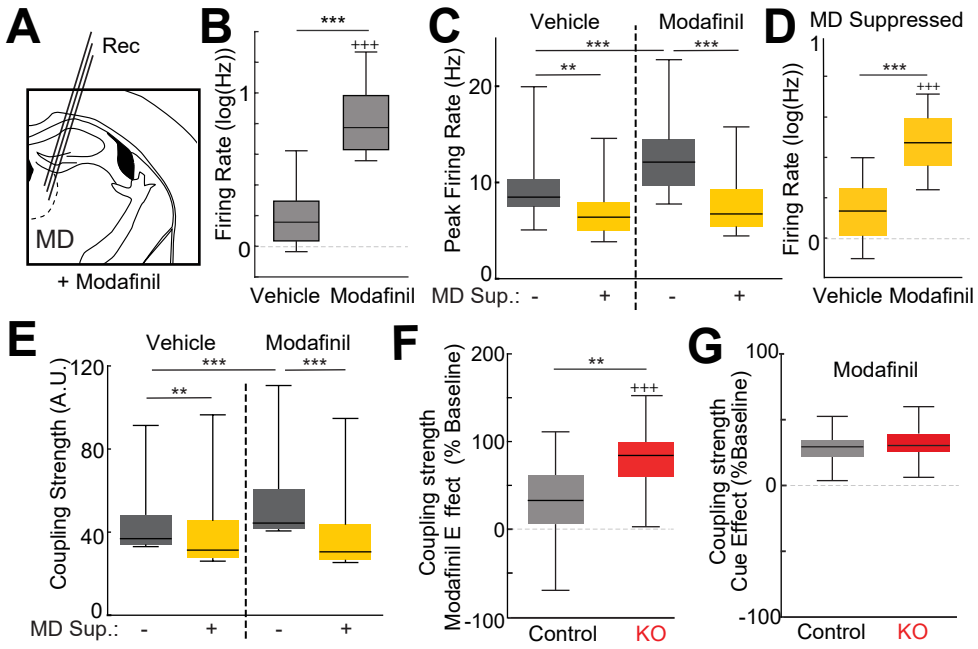

Figure S5: Modafinil increases functional connectivity in the PFC through an MD dependent mechanism. Related to Figure 5

A. Schematics for MD recording outside the task with modafinil administration. **B.** Quantification of average firing rates in the MD following vehicle or modafinil injections. Modafinil increased firing rate above baseline and vehicle injection (N=2 mice, n = 159 neurons; ***p < 0.001 pairwise sign-rank test, +++p < 0.001 comparison with baseline). **C.** Evoked peak firing rate across responding neurons with and without optogenetic suppression of MD following administration of vehicle or modafinil. This recording was performed outside the task. Evoked firing was significantly reduced by MD suppression and increased by modafinil administration (p < 3.6x10-25 MANOVA Main Effects of suppression, 1.9x10-16 Interaction; N = 2 mice, 155 neurons; **p < 0.005, ***p < 0.001 pairwise rank-sum test). **D.** Increase of spontaneous activity in PFC by modafinil was not affected by suppressing MD. This recording was performed outside the task. (N = 2 mice, n = 155 neurons, *** p < 0.001 pairwise rank-sum test, +++ p < 0.001 comparison with baseline) **E.** Coupling strength across neurons with and without optogenetic suppression of MD following administration of vehicle or modafinil outside the task. Coupling was significantly reduced by MD suppression and increased by modafinil administration (p < 1x10-80 MANOVA Main Effect of suppression p < 1.0x10-32 Interaction; N = 2 mice, n = 155 neurons; **p < 0.005, ***p < 0.001 pairwise rank-sum test) **F.** Quantification of the increase of coupling strength by modafinil administration between PFC neurons in control mice (4 mice, n = 863 neurons) and in KO (4 mice, n = 947 neuron). Average strength in both cued and uncued trials are plotted. (p < 1.8x10-13 MANOVA; +++ p<0.001 comparison with baseline, **p < 0.01 pairwise sign-rank test) **G.** Quantification of the effect of cue on the coupling strength after modafinil administration between control and KO PFC neurons. (N = 4 control and 4 KO mice, n = 863 control and 947 KO neurons; pairwise rank-sum test)

Boxplots: median (line), quartiles (box), 95% confidence interval (whiskers)

FigureS6 related to Figure6

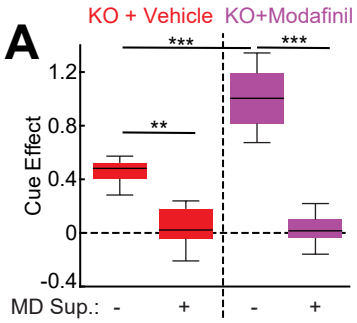

Figure S6: Behavioral improvements in cued auditory discrimination after modafinil administration were MD dependent. Related to Figure 6

A. Behavioral improvement on trials in which a noise predicting cue was presented (Cue Effect) on difficult trials (SNR 3.2) for KO mice. Box plots show cue effect with and without optogenetic suppression of the MD either following injection of vehicle (red, left) or modafinil (purple, right). The cue effect was significantly reduced by MD suppression and this manipulation also eliminated modafinil-dependent improvement (N=4 mice, 12 sessions per condition, p=3.9x10-6, MANOVA Main Effects, p=0.001 Interaction; **p<0.01, ***p<0.001, pairwise rank-sum test with Bonferroni correction).

Boxplots: median (line), quartiles (box), 95% confidence interval (whiskers)